Modeling flow liquefaction, its mitigation, and comparison with centrifuge tests

E. Naesgaard[1], P. M. Byrne[1], M. Seid-Karbasi[1], and S.S. Park[1]
[1]*Department of Civil Engineering, University of British Columbia, Vancouver, Canada*

Abstract

There is a common misconception among practicing engineers that loose sand soils behave in an undrained manner during earthquake loading. Recently it has been demonstrated that pore water flow and pressure redistribution which occurs during and following earthquake shaking may result in relatively thin zones with very high void ratio, or in the extreme, water inter-layers, immediately below low permeability layers. These high void ratio/water inter-layer zones have very low to near zero shear strength, much lower than obtained from undrained laboratory element tests. Without a low permeability barrier to retard the escape of groundwater, flow liquefaction generally does not occur, even for loose sands on relatively steep slopes subjected to strong shaking. A program of simple shear and centrifuge testing was carried out to calibrate a numerical model. Flow failure with post-shaking localized shear immediately below a low permeability barrier was modeled in the centrifuge and emulated in the numerical analyses. Procedures for numerically modeling the flow liquefaction and localization under the barrier are discussed. The analyses demonstrate that the strength reduction effects of the low permeability barrier can be captured by the numerical analyses and that drainage slots are an effective means of mitigating flow deformations.

Keywords— *Centrifuge, earthquake, flow, liquefaction, numerical, pore water, redistribution*

INTRODUCTION

Numerous flow failures have occurred during or following strong earthquake shaking when liquefaction is triggered [1][2][3][4]. These flow liquefaction failures are deemed to occur when the static driving stress exceeds the soil shear strength. Shear strength of soil following triggering of liquefaction has been called residual strength, and has commonly been assumed to be an undrained strength parameter. Seed [3] back-calculated these strengths from case histories while others [5] attempted to determine them from laboratory tests. Recent work [6][7][8][1][9][10] has shown that the undrained assumption is not correct and may be unconservative. They have demonstrated that pore water flow and pressure redistribution which occurs during and following earthquake shaking may result in relatively thin zones with very high void ratio, or in the extreme, water inter-layers, below low permeability layers. These high void ratio/water inter-layer zones have very low to near zero shear strength, much lower than obtained from undrained laboratory element tests. Without a low permeability barrier to retard the escape of groundwater, and/or some form of soil mixing, flow liquefaction generally does not occur, even for loose sands on relatively steep slopes subjected to strong shaking.

A constitutive model, UBCSAND, and analysis procedure has been developed at the University of British Columbia for modeling the behavior of sandy soils during earthquake shaking; including the modeling of liquefaction triggering and related deformations [12]. A program of cyclic simple shear and dynamic centrifuge testing has recently been carried out specifically for the purpose of calibrating the numerical model.

This paper examines the flow liquefaction modeling aspects and procedures for mitigating the effects of low permeability barriers within sand soil deposits. The constitutive model, analysis procedures and comparison of numerical analyses and centrifuge test predictions are described.

SOIL LIQUEFACTION AND PORE WATER REDISTRIBUTION OVERVIEW

When typical loose sand, D_r = 40% is tested in the laboratory in drained cyclic simple shear it is initially contractive on loading and unloading. However at large strains in loading the soil becomes dilative when the stress state exceeds the constant volume friction angle, φ_{cv}. Dense sand behaves in a similar manner except the dilative response is much more pronounced. Both soils are always contractive on unloading. The net result of cyclic loading is generally a reduction in sample volume.

If the pores are filled with water that is prevented from escaping the sample (undrained condition), then pore pressures increase when the soil skeleton attempts to contract and decrease when the soil skeleton attempts to dilate. As pore pressure builds up the effective stress and shear strength decreases, however with attempted dilation the effective stress and shear strength increases. Dilative response is deemed to occur when the stress path exceeds the phase transformations or φ_{cv} line. With repeated cycles the stress path may reach the zero effective stress / zero shear strength origin and true liquefaction occurs. However upon continued monotonic shearing to large strains the soil will dilate, moving up the failure envelope gaining strength and the so-called *residual strength* will not be reached until, (i) the pore-water cavitates and thus allows the sample to increase in volume and reach the steady state, or (ii) the high mean effective stress

generated by dilation suppresses the dilation and the soil reaches its critical state strength, or (iii) the sand grains crush and the soil reaches a critical state of the crushed material. The strength of the sand reached in (i), (ii) or (iii) is generally much higher than the commonly accepted 'undrained" residual strengths back-calculated from case histories [13], and is likely much higher than the drained strength.

If, in lieu of undrained loading, a small inflow of water is allowed to occur, it will reduce or eliminate the strength gain resulting from expansion [6]. If the inflow volume exceeds the expansion due to shear induced dilation then the soil quickly reaches the state of zero effective stress and has truly liquefied.

There are numerous case histories where soil liquefaction occurred during earthquake shaking but related flow failure did not occur until some time after end of shaking. The classical examples are the Lower San Fernando Dam [3] and in Niigata eyewitnesses reported that the girders of the Showa Ohashi Bridge began to fall a few minutes after the earthquake motion had ceased [2].

Natural and many man-made soils are often layered and have variations in grain-size and related permeability throughout the deposit. Earthquake shaking and related liquefaction will induce a generally upward gradient and pore-water flow. When there is a low permeability layer or barrier, the upward migrating pore water gets trapped under or within the bottom portion of the barrier and forms an interface with low effective stress. At the limit an actual water interlayer with zero shear strength will develop.

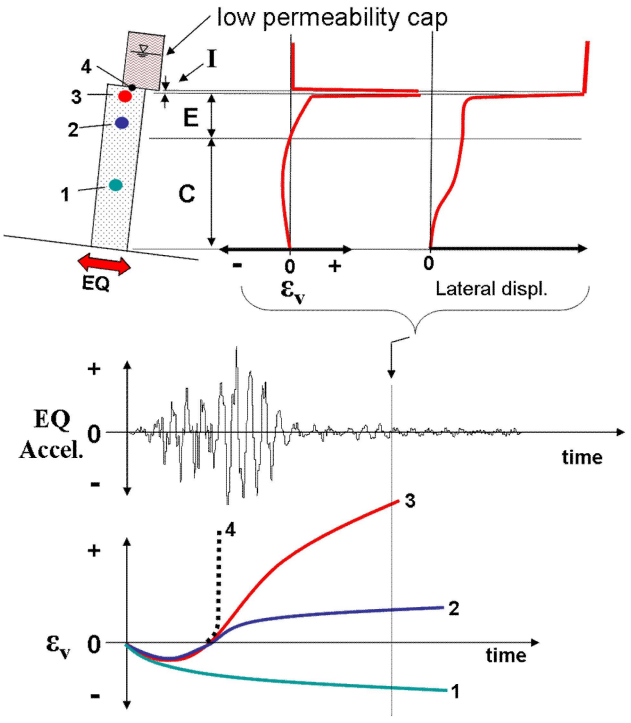

Fig. 1 Volumetric strain (ε_v) within an infinite slope column with a low permeability crust over loose sand

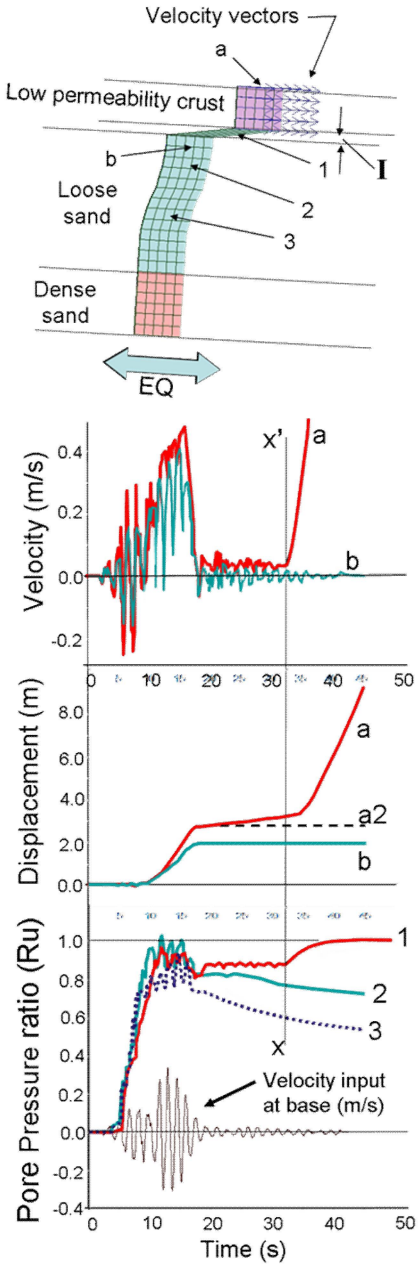

Fig. 2 Infinite slope (1D) column with low permeability barrier cap. At time x-x' zone 'I' has expanded to the critical state, dilation goes to zero, and flow failure is initiated.

ANATOMY OF A LOOSE SAND LAYER UNDERLYING A LOW PERMEABILITY BARRIER

Based on numerical analysis of a one dimensional column with a small static bias, [10] showed that the loose soil, of thickness 'L' underlying a low permeability barrier consists of three zones: a lower contractive-zone (Zone 'C'), an upper expansive zones (Zone 'E'), and a thin very expansive interface layer (Zone 'I') at the top (Fig. 1 & 2).

At the onset of earthquake shaking Zones 'E' and 'I' have not developed and the full depth of soil is

contractive. However with time, pore water flows upward from the lower layer 'C' and expansive Zones 'E' and 'I' develop. The blockage effect on flow caused by the presence of the barrier causes the highest rate of expansion to occur directly beneath the barrier. This is important as this causes localization and formation of a thin very weak layer at the interface. The dilation or expansion within zone 'E' and 'I' is due to a combination of dilation induced by the static shear bias and, more importantly, by the influx of water from Zone 'C' below.

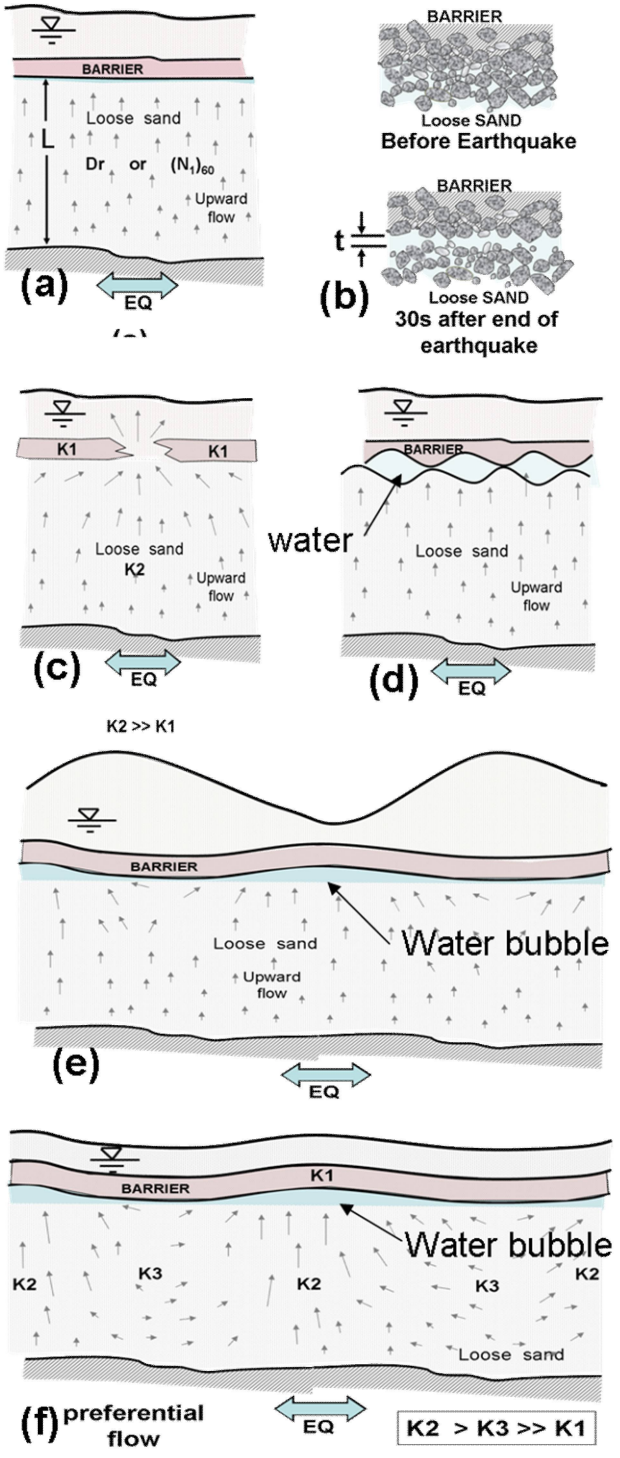

Fig. 3. Factors affecting the thickness and residual strength of the localized shear zone underlying a low permeability barrier (a) density & thickness L, (b) grainsize, (c) continuity and permeability of barrier, (d) interface roughness, (e) total stress variation, and (f) preferential flow paths.

If zone 'I' is thought of as a very thin soil element, with plane boundaries, then a small influx of pore water will cause a large volumetric strain at the barrier. This will result in the element quickly going to the critical state with zero effective stress and zero shear strength. Further inflow will cause localization and formation of a water film or interlayer. Further shearing will not induce dilation. The strength will remain zero until the excess pore water drains.

If the soil has a static shear bias the zone 'I' layer will attempt to fail prior to reaching the critical state and zero strength. This may cause dilation, which in turn may cause a temporary drop in pore pressure and related strength increase. However with continued inflow the layer quickly reaches the critical state and any further inflow leads to zero effective stress and zero shear strength.

In real soils the boundary of Zone 'I' will not be perfectly plane, infinitely thin or of infinite lateral extent but will have undulations, varying normal stresses, finite grain sizes, etc. These items will result in the 'residual' shear strength along the interface varying both in time and space with an average value that is greater than zero. Some items that influence the shear strength of the barrier interface (Zone 'I') include:

1) *Net volume of inflow*: The volume of inflow will be a function of the thickness of the loose layer, relative density of the loose layer, drainage conditions (whether essentially vertical 1D drainage conditions or combined vertical and lateral drainage), and earthquake shaking amplitude and duration (Fig. 3a). The greater the irregularities, undulations, etc. of the interface layer the greater the net inflow required to achieve zero effective stress.

2) *Grain-size*: The grain-size of zone I will have an effect on the dilation required in order to reach the critical state. The larger the grains the greater the inflow required for steady state shear to be achieved (Fig. 3b).

3) *Permeability and continuity of the barrier*: Leakage through the barrier will reduce the net inflow into the interface and therefore will reduce the effectiveness of the barrier (Fig. 3c).

4) *Boundary undulations*: Undulations in the boundary of the barrier layer will affect the volume of inflow required to achieve zero strength (Fig. 3d). These may be undulations that precede the earthquake shaking and/or may be due to deformations induced by strong earthquake shaking.

5) *Variations in vertical stress*: Variations in vertical stress along the barrier boundary will allow the higher stressed sections to maintain some strength while the lower stressed sections heave (Fig. 3e)

6) *Concentration of groundwater seepage*: The upwelling groundwater may be preferentially

concentrated (Fig. 3f) due to variations in permeability and discontinuities within the ground.

7) *Soil Frictional properties*: The frictional properties of portions of the barrier that do not have zero strength will affect the average strength.

The "residual strength" that is back-calculated from case histories [13] may approximately represent the average shear strength of the interface layer at the time of failure. This 'residual strength' is dependent on many parameters in addition to the normally assumed $(N_1)_{60}$ of the loose layer [9].

NUMERICAL MODELING OF PORE WATER REDISTRIBUTION AND FLOW LIQUEFACTION

Much of the behavior of the pore water redistribution and flow liquefaction behavior can be captured using an appropriate numerical program. Desirable features for the program include:

a) An effective stress constitutive model with coupled mechanical stress-strain – pore water flow features.
b) A mechanism to account for the localization that occurs adjacent to the low permeability barrier interface.
c) The model should capture the drained and undrained behavior of element tests with similar stress paths to that expected in the field during earthquake loading. This should include capturing shear induced contraction and dilatancy, and ability to model inflow tests.
d) The model should be relatively simple and only require a limited number of input parameters that can be determined from commonly available field and laboratory tests.
e) The model should be able to emulate the behavior of field case histories and/or centrifuge tests.

Item (b) above is problematic. Localization means that the behavior will be element size dependent. The localization of the barrier interface could be modeled by (i) using many very small elements; (ii) the use of larger elements with a dilation cut-off (iii) an interface with a dilation cut-off, or (iv) by using a total stress residual strength immediately below or within the barrier for the latter portion of the numerical analysis. Each of these is discussed in more detail below.

The alternatives for numerically modeling the barrier interface and related localization

(i) *Use very small elements in vicinity of barrier*: Very small elements with a function that sets dilation to zero when the critical state void ratio is reached would model the localization in a realistic manner. Grain size, boundary undulations, and other barrier properties could be physically modeled with the very small elements. The down side is that the very small elements make most existing programs excessively slow and impractical.

(ii) *Large element with dilation cut-off*: A large element can be tricked into behaving like a small element by having a function that 'kills' dilation at a pre-specified void ratio or volumetric expansion of the element. As illustrated in Fig. 4, this pre-specified volumetric expansion is much less than that required to get the whole element to the true critical state. The volume of inflow permitted prior to 'killing' dilation would be a function of the material grain size, boundary undulations, etc. and could be approximated from the back-calculation of case-histories and centrifuge tests.

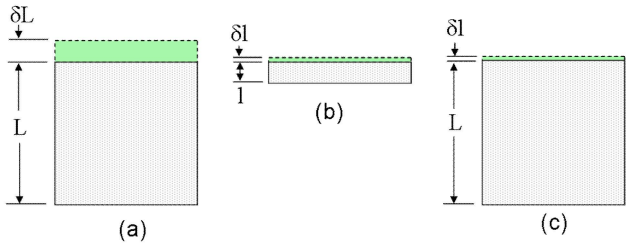

Fig 4. Large element(c) emulating the behavior of a small element (b). If (a) and (b) are at critical state with $\delta l/l = \delta L/L$ then (c) can be made to behave similar to (b) by setting dilation to 0 when the volumetric strain is equal to $\delta l/L$.

(iii) *Numerical interface with no dilation*: A numerical interface could be used to model the layer underlying a barrier. This interface could have simple Mohr Coulomb frictional properties with no dilation. The shear strength on the interface would go to zero when the effective stress was zero. The behavior of the interface would be similar to an infinitely thin element. The surface of the interface could be undulated to model irregularities in the barrier.

(iv) *Switch the element or numerical interface to a total stress 'residual strength'*: An alternative to using a dilation cut-off or an interface with no dilation would be to change the soil properties, at an appropriate time (possibly end of strong shaking), within the layer underlying the barrier layer, or the barrier layer itself, from effective stress to a total stress 'residual strength'. Volumetric strain (similar to that used to trigger dilation-cut-off in (iii) above could be used to trigger when to change to the strength within the layer to the total stress residual strength value. If the residual strength is less than the static driving stress then a flow deformations would occur. Note that this is different than the current practice of changing the properties of the whole loose sand layer to the residual strength when liquefaction is triggered. In the proposed procedure the residual strength would only be used in the barrier elements, elements immediately below the barrier, or the barrier interface. The remainder of the loose sand elements would still use the effective stress constitutive model. The residual strength selected would have to be tied to case histories and would be similar to that proposed by [13] & [14].

NUMERICAL ANALYSES

Numerical analyses of simple shear laboratory tests, 1-D soil columns, and centrifuge tests with low

permeability barrier layers, has been conducted as part of the UBC – C-Core Liquefaction Initiative. The effective stress constitutive model UBCSAND [15][12], running in commercially available finite difference program FLAC [16], was used for the analyses.

The UBCSAND constitutive Model

UBCSAND is an elastoplastic effective stress model with the mechanical behavior of the sand skeleton and pore water flow fully coupled. The model includes a yield surface related to the developed friction angle, non-associative flow rule, and definitions for loading, unloading, and hardening. A hyperbolic relationship is used between stress ratio and plastic shear strain. 2% Raleigh damping is used with the UBCSAND model to provide energy dissipation at small strain levels. Key elastic and plastic parameters used are adjusted so as to give a good match with simple shear laboratory tests as the loading path of this test, including rotation of principal stress axes, closely approximates that which occurs during earthquake loading. A series of simple shear tests, including cyclic drained and undrained tests with and without static bias, and monotonic drained and undrained tests were conducted for this purpose [17]. Fig. 5 shows a typical comparison of a simple shear test result to that predicted by the UBCSAND model. Reference [18], showed that the model could also emulate the behavior of triaxial tests with fluid inflow [6].

During the dynamic analysis the pore pressures are generated by shear induced plastic volume change. This

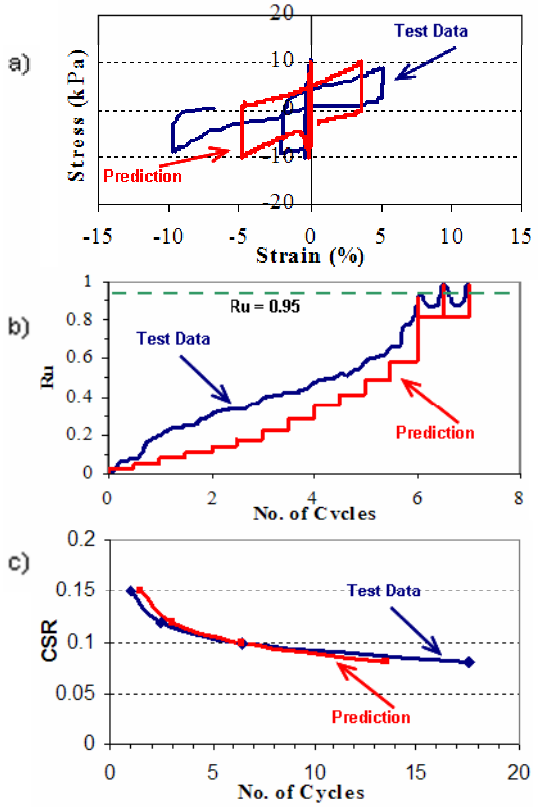

Figure 5. Comparison of undrained simple shear tests to UBCSAND predictions [10][17]

reduces mean effective stress and initiates pore water flow from zones of high head to low head. Volumetric strain is monitored in each element and when a pre-set strain is reached dilation in the element is set to zero (this threshold will typically only be reached when the element is underlying a low permeability barrier).

When the grid is submerged, water is modeled as an applied pressure to the top of the mesh. This pressure has to be updated periodically during the dynamic analyses in order for the applied pressure to be compatible with grid deformations.

The pore pressure in a FLAC element is the average of the nodal values. Therefore low permeability layers have to be at least two elements thick if high pore pressures are to be achieved within the underside of the barrier. Localization was accounted for by using a volumetric expansion dilation-cut-off. For a one meter thick element the dilation was set to zero when a volumetric expansion strain of 0.005 was reached. This seemed to give reasonable correlation with centrifuge test results. However this value is preliminary and further calibration work is required.

1D Analyses

Infinite slope 1D numerical analyses are useful for developing insights into the behavior of the low permeability barrier and flow slide mechanisms. Figs. 1 and 2 illustrate a typical 1D column analysis with typical volumetric strain time histories at various locations within the column. Fig. 2 shows a displaced grid with velocity time histories above and below the barrier. Note how a flow slide or flow failure condition is initiated (increasing velocity) at time x-x'. This is the critical state when shear induced dilation goes to zero. Shear strain is concentrated (localized) immediately below the low permeability barrier, and the flow failure is independent of the inertial forces from strong shaking.

Analyses of centrifuge tests with and without impermeable barrier

A series of eight centrifuge tests were carried out at the C-CORE facility in Newfoundland [20][21]. The centrifuge tests modeled submerged slope configurations with and without: low permeability silt barrier, soil densification dyke, and drainage trenches. Air pluviated Fraser River sand with a relative density of approximately 40% and minimum and maximum void ratio of 0.62 and 0.94 was used. Non-plastic commercial ground silica silt was used for the low permeability barrier and clear uniform coarse sand was used for the drainage layers. D_{10} and D_{50} for the loose sand was 0.16 mm and 0.26 mm, for the silt was 0.005 mm and 0.016 mm, and for the drainage sand was 2.2mm and 2.9 mm respectively. The centrifuge tests were at 70g with a water plus hydroxypropyl-methylcellulose fluid with a viscosity of 35 times that of water. Simulated earthquake motion was applied during flight using a hydraulically actuated shaker. All dimensions, time histories, etc. given in this paper are in the scaled prototype dimensions rather than the actual

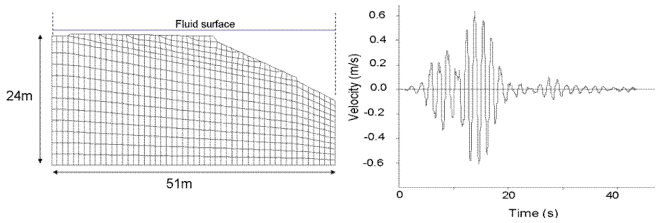

Fig. 6. Grid and time velocity time history used for centrifuge predictions

centrifuge dimensions. During centrifuge spin-up there are large changes in effective stress which result in 'stress densification' of loose sandy soils [19]. This was accounted for in the analyses. A typical grid and input earthquake record is shown in prototype scale in (Fig. 6). The side forces that would occur within the centrifuge box were accounted for during the dynamic analysis by applying internal nodal forces that were a function of the out-of-plane effective stress (σ'_z) times the sidewall friction coefficient. Normalized velocities were used to give the direction of the internal nodal forces.

Liquefaction flow failure was observed in the tests which included the low permeability silt barrier and higher levels of shaking. Flow failure generally did not occur when the barrier was absent or if drainage trenches were placed through the barrier. Similar behavior has been observed by others [8][1][9].

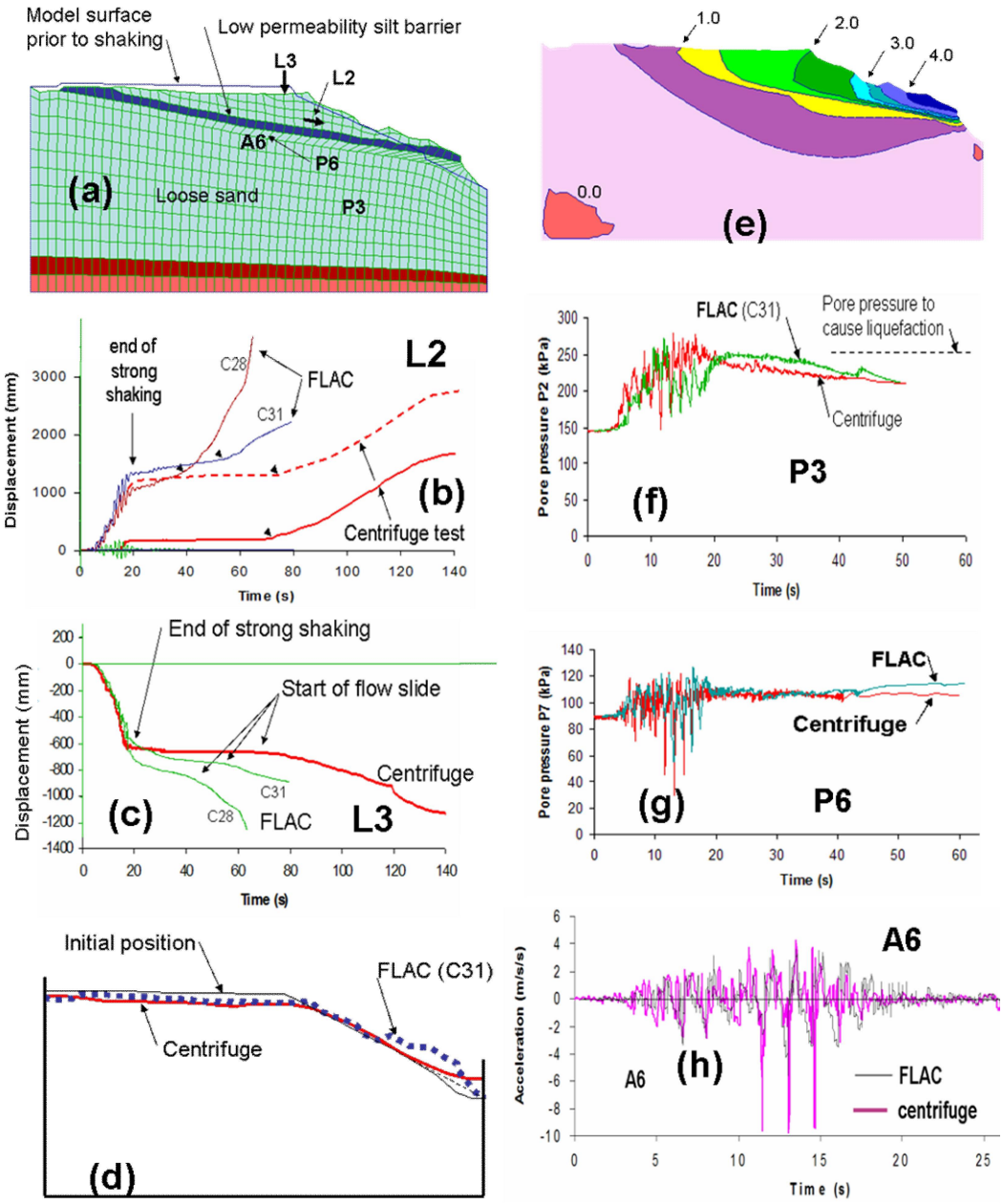

Fig. 7. Comparison of Centrifuge tests and numerical results for profile with low permeability silt barrier (COSTA-C). (a) displaced grid, (b) Horizontal displacement of sliding block over barrier (for the centrifuge data the solid line is measured & the dashed line is corrected to better match final displacements), (c) vertical displacement at crest, (d) centrifuge & numerical surface profiles, (e) calculated lateral displacement contours in meters, (f) & (g) pore pressure time histories at P3 & P6, (h) acceleration time history at A6.

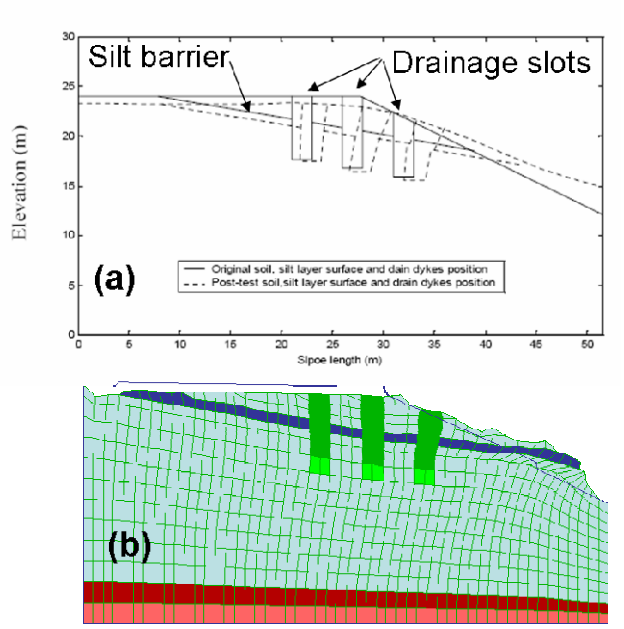

Fig. 8. (a) Initial and displaced profile of centrifuge test CT5 with three drainage slots (b) numerical analysis of same.

Fig. 7 compares centrifuge and numerical results for the COSTA-C test [20] that included a low permeability barrier. In the COSTA-C test a flow slide occurred at the barrier interface at approximately 50s after end of strong shaking. Figs. 8 shows displaced profiles for a similar model, CT5 [21] that had permeable drainage slots through the silt barrier. With drainage slots (Figs. 8 & 9) all deformation occurred during strong shaking (t<20s) and flow deformation is prevented.

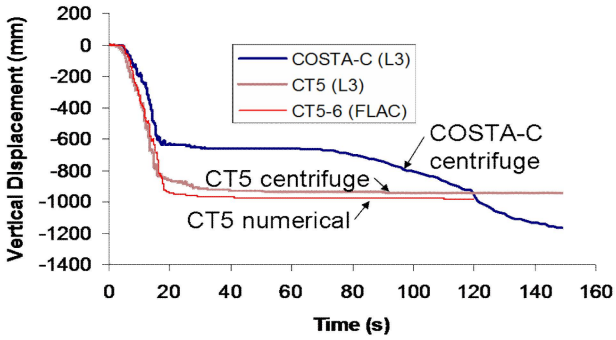

Fig. 9. Comparison of vertical displacement near crest with (CT5) and without (COSTA-C) drainage slots. Post-shaking flow initiated in the COSTA-C test at approximately 70s.

MITIGATION OF FLOW LIQUEFACTION

As illustrated in Fig. 9, drainage is an effective means of mitigating low permeability barrier induced flow sliding. However, even with drains significant deformations may still occur during strong shaking, but post-shaking flow movements do not occur. If the movements induced during heavy shaking are of concern then ground densification, possibly combined with drainage measures, or use of dowels combined with drains could be considered. These suggested ground improvement measures are schematically illustrated on Fig. 10. Mitigation with relief wells (drains) only (Fig. 10(b)) will prevent the occurrence of flow slides but large movements may still occur during strong shaking. Ground densification alone will reduce movements during strong shaking however post-shaking migration of pore water may lead to weak zones. Combining ground densification with some relief wells (Fig. 10(c)) is an optimum solution as it reduces movements during strong shaking and prevents pore pressure build-up within the densified block. Piles may be used as dowels and for compaction. This is useful in interlayered silt and sand soils that do not respond well to normal densification methods. Inclusion of relief wells between the piles (Fig. 10(d)) improves the performance by mitigating pore pressure build-up.

One of the strengths of numerical analyses is the ability to assess the effectiveness of various mitigative measures and the ability to optimize the designs by conducting parametric analyses. Numerical analyses also bring considerable insight on behavior mechanisms. This procedure was used for the seismic upgrade design of George Massey tunnel in Greater Vancouver, British Columbia [22][23]. The 1.5 km long submerged-tube tunnel underlies the Fraser River and is buried in loose liquefiable sand. Effective stress numerical analyses were used to demonstrate that drains and densification placed adjacent to the tunnel could mitigate excessive upward and lateral tunnel displacements. Good correlation was obtained between the numerical analyses and those from centrifuge tests made to calibrate the model. Construction of the seismic upgrade measures is currently in progress.

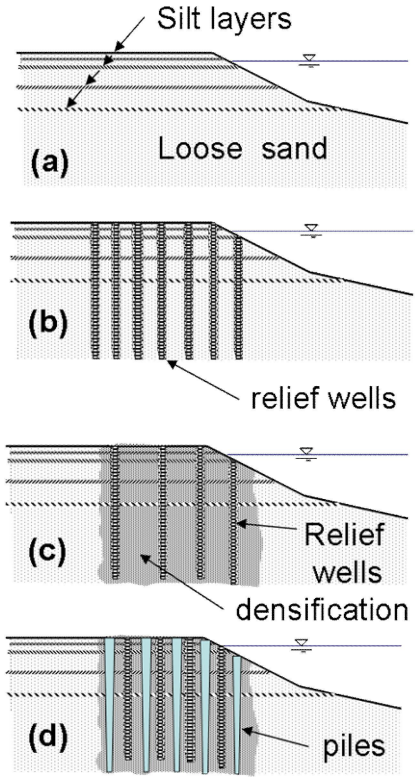

Fig. 10. Mitigation schemes for hypothetical water edge with low permeability silt layers

CONCLUSIONS

The Liquefaction induced displacements and flow failures observed in the centrifuge tests have been successfully simulated numerically using the UBCSAND model within the commercially available program FLAC. UBCSAND is an effective stress model with full coupling between mechanical behavior and groundwater flow.

Special features in the numerical model for the back-analyses of the centrifuge tests include: allowance for stress densification during spin-up, allowance for variation in fluid modulus with saturation and confining pressure, inclusion of internal force vectors to account for side friction within the centrifuge container, and a volumetric-strain-triggered-dilation-cut-off to account for the localization or element size effects that occur immediately below the low permeability barrier.

This paper examines the flow liquefaction modeling aspects and procedures for mitigating the effects of low permeability barriers within sand soil deposits. The constitutive model, analysis procedures and comparison of numerical analyses predictions to those of the centrifuge tests are described. One of the strengths of numerical analyses is the ability to assess the effectiveness of various mitigative measures and the ability to optimize the designs by conducting parametric analyses. Numerical analyses also bring considerable insight on behavior mechanisms.

The inclusion of drains through the low permeability layers is shown to be an effective measure for mitigation of post-earthquake flow failure.

ACKNOWLEDGMENTS

The authors acknowledge the support from the Ministry of Transportation UBC Professional Partnership program, the Canadian Council of Professional Engineers, Trow Associates Inc., and the National Scientific and Engineering Research Council through Strategic Liquefaction Grant No. NSERC 246394, and NSERC COSTA No. 03608-CG068625. Centrifuge tests were conducted by Ryan Phillips, Minqiang Tu, and Stephen Coulter at C-CORE, and their expertise and assistance is appreciated. Laboratory testing by D. Wijewickereme & S. Sriskandakumar was an integral part of the work.

REFERENCES

[1] Kokusho, T., "Current state of research on flow failure considering void redistribution in Liquefied deposits," *Soil Dynamics and Earthquake Engineering* 23, 585-603, 2003.

[2] Hamada, M., "Large ground deformations and their effects on lifelines: 1964 Niigata Earthquake" *Proc., Lifeline Performance during Past Earthquakes, V. 1: Japanese Case Studies Tech. Rep NCEER-92-0001,* Buffalo, N.Y., 3/1-3/123, 1992.

[3] Seed, H.B., "Design problems in soil liquefaction," *J. Geotechnical Eng. Div., ASCE*, Vol. 113, No.8, 827-845, 1987.

[4] Ishihara, K., "Post-earthquake failure of a tailings dam due to liquefaction of the pond deposit," *Proc. Inter. Conf., Case Histories in Geotechnical Engineering*, Rolla, Missouri, V. 3, pp. 1129-1143, 1984..

[5] Poulos, S.J., Castro, G., and France, W., "Liquefaction evaluation procedure," *J. Geotechnical Engineering Div., ASCE*, Vol. 111, No.6, pp. 772-792, 1985.

[6] Vaid, Y.P., and Eliadorani, A., "Instability and liquefaction of granular soils under undrained and partially drained states," C*anadian Geotech. J.* Vol. 35, pp. 1053–1062, 1998.

[7] Yoshida, N., and Finn, W.D.L., "Simulation of liquefaction beneath an impermeable surface layer," Soil Dyn. Earthquake Eng. 19, pp. 333-338, 2000.

[8] Kokusho, T., "Water film in liquefied sand and its effect on lateral spread," *J. Geotech. Geoenviron. Eng.* 125(10), pp. 817–826, 1999.

[9] Kulasingam, R., Malvick, E.J., Boulanger, R.W., and Kutter, B.L., "Strength loss and localization of silt interlayers in slopes of liquefied sand," *J. of Geotech. Geoenviron. Eng., ASCE,* Vol. 130, No. 11, November 1, pp. 1192-1202, 2004..

[10] Seid-Karbasi, M., and Byrne, P.M., "Liquefaction, lateral spreading and flow slides," Proc. 57th Canadian Geotechnical Conf., Session 2c, pp. 23-30, 2004.

[12] Byrne, P.M., Park, S.S., Beaty, M., Sharp, M., Gonzalex, L., Abdoun, T., "Numerical modeling of dynamic centrifuge tests," *13th World Conference on Earthquake Engineering, Vancouver, B.C.*, paper 3387, 2004.

[13] Seed, R.B., and Harder, L.F., Jr., "SPT-based analysis of cyclic pore pressure generation and undrained residual strength.," *In* Proc. of the H.B. Seed Memorial Symposium, Bi-Tech Publishing Ltd., Vol. 2, pp. 351–376, 1990.

[14] Olson, S. M. and Stark, T. D., "Liquefied strength ratio from liquefaction flow failure case histories," Canadian Geot. J., Vol 39, pp. 629–647, 2002.

[15] Beaty, M., and Byrne, P.M., "An effective stress model for predicting liquefaction behaviour of sand," Geotechnical Earthquake Engineering and Soil Dynamics III. P. Dakoulas, M. Yegian, and R Holtz (eds.), ASCE, Geotechnical Special Publication 75 (1), pp. 766-777, 1998.

[16] ITASCA "FLAC - Fast langrangian analysis of continua, Version 4.0 ITASCA Consulting Group Inc., Minneapolis, Minnesota, 2002.

[17] Sriskandakumar, S., "Cyclic loading response of Fraser River sand for numerical models simulating centrifuge tests," M.A.SC. Thesis, Civil Eng. Dept., University of British Columbia, Vancouver, B.C., 2004.

[18] Atigh, E. and Byrne, P.M., "Liquefaction flow of submarine slopes under partially undrained conditions: an effective stress approach," *Canadian Geotech. J.*, V. 41, pp. 154-165, 2004.

[19] Park and Byrne, "Stress densification and its evaluation," 2004, Canadian Geotech.l J., *Vol.41(1), pp. 181-186,* 2004.

[20] Phillips, R., and Coulter, S., "COSTA-C Centrifuge Test Data Report", C-CORE Report R-04-082-075, January, 2005.

[21] Phillips, R.,, Tu, M., and Coulter, S., "C-CORE. Earthquake Induced Damage Mitigation from Soil Liquefaction. Data report – Centrifuge Test CT5". Contract Report Prepared for University of British Columbia. C-CORE Report R-04-068-145, December, 2004.

[22] Naesgaard, E., Yang, D., Byrne, P.M. and Gohl, B., "Numerical analyses for the seismic safety retrofit design of the immersed-tube George Massey Tunnel," *Proc. 13th World Conf. on Earthquake Engineering*, Vancouver, paper 112, August, 2004.

[23] Yang, D., Naesgaard, E., and Gohl, B. "Geotechnical seismic retrofit design of George Massey Tunnel." *Proc. 12th Pan-American Conf. on Soil Mechanics and Geotech.l Eng., Cambridge*, USA, June 22-26, pp. 2567 – 2574, 2003,